

Orbital Maneuvering System Design and Performance for the Magnetospheric Multiscale Formation

A photograph of a large satellite stack, likely the Magnetospheric Multiscale Formation, positioned between two large cylindrical tanks. The stack consists of several rectangular modules connected vertically. The tanks on either side have numerous horizontal bands and small rectangular ports. The background shows the interior of a clean room with white walls and ceiling support structures.

AAS 15-815

Steven Queen, Dean Chai, and Sam Placanica

NASA/Goddard Space Flight Center, Code 591

AAS/AIAA Astrodynamics Specialist Conference

August 13, 2015





MMS Mission Overview

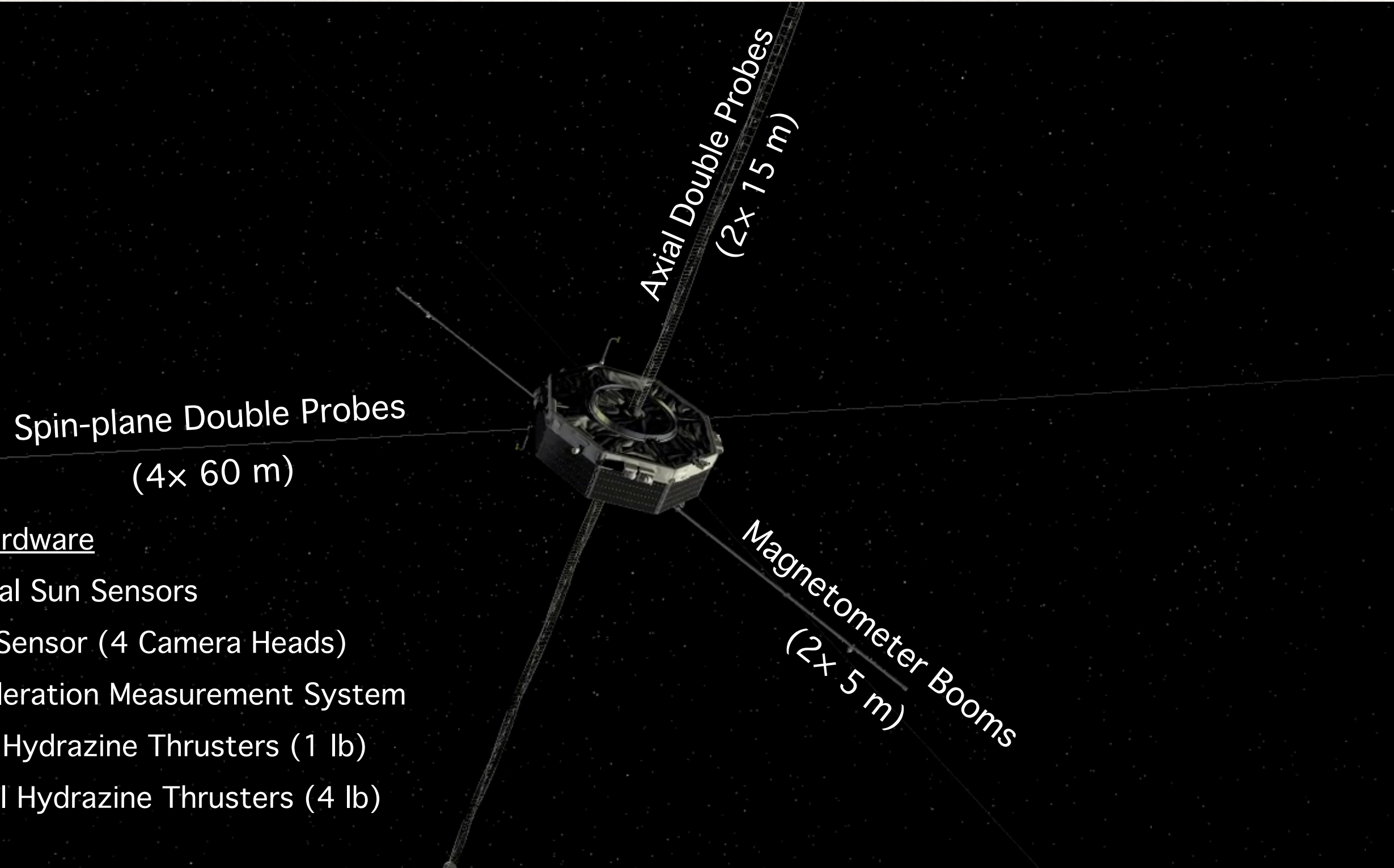
Spin-plane Double Probes
(4x 60 m)

Axial Double Probes
(2x 15 m)

Heliophysics Objective — observe geomagnetic reconnection
Four observatories that form a tetrahedron near apogee



MMS Mission Overview





Performance Requirements

Once in science mission orbits, the four 0.12-km diameter observatories plan to form a tetrahedron with as little as 4-km of separation between spacecraft.

- The stated operational goal of maneuvering the fleet is no more often than once every two weeks (on average)
- Derived maneuvering accuracy requirement levied on the ACS

Maneuver Size (m/sec)	Error Allocation (3σ)	
	Magnitude	Direction*
0 – 0.05	5 mm/sec	$40^\circ \rightarrow 5^\circ$
0.05 – 0.10	1%	$5^\circ \rightarrow 1.5^\circ$
$0.10 <$	1%	1.5°

* (\rightarrow indicates linear decrease vs. size)



Attitude and Rate Estimation

Attitude and rate are derived from the μASC Star Tracker System, provided by the Technical University of Denmark

- Four camera head units (CHU)
- 4 Hz update rate
- Measurements combined in a Multiplicative Extended Kalman Filter (MEKF)

Image from MMS-3, CHU-B



MEKF Error State Dynamics

$$\begin{bmatrix} \dot{\alpha} \\ \dot{\delta\omega} \end{bmatrix} = \begin{bmatrix} -\hat{\omega}^{\times} & \mathbb{I} \\ 0 & I^{-1} \left[(I\hat{\omega})^{\times} - \hat{\omega}^{\times} I \right] \end{bmatrix} \begin{bmatrix} \alpha \\ \delta\omega \end{bmatrix} + \begin{bmatrix} 0 \\ I^{-1} \end{bmatrix} u + w$$



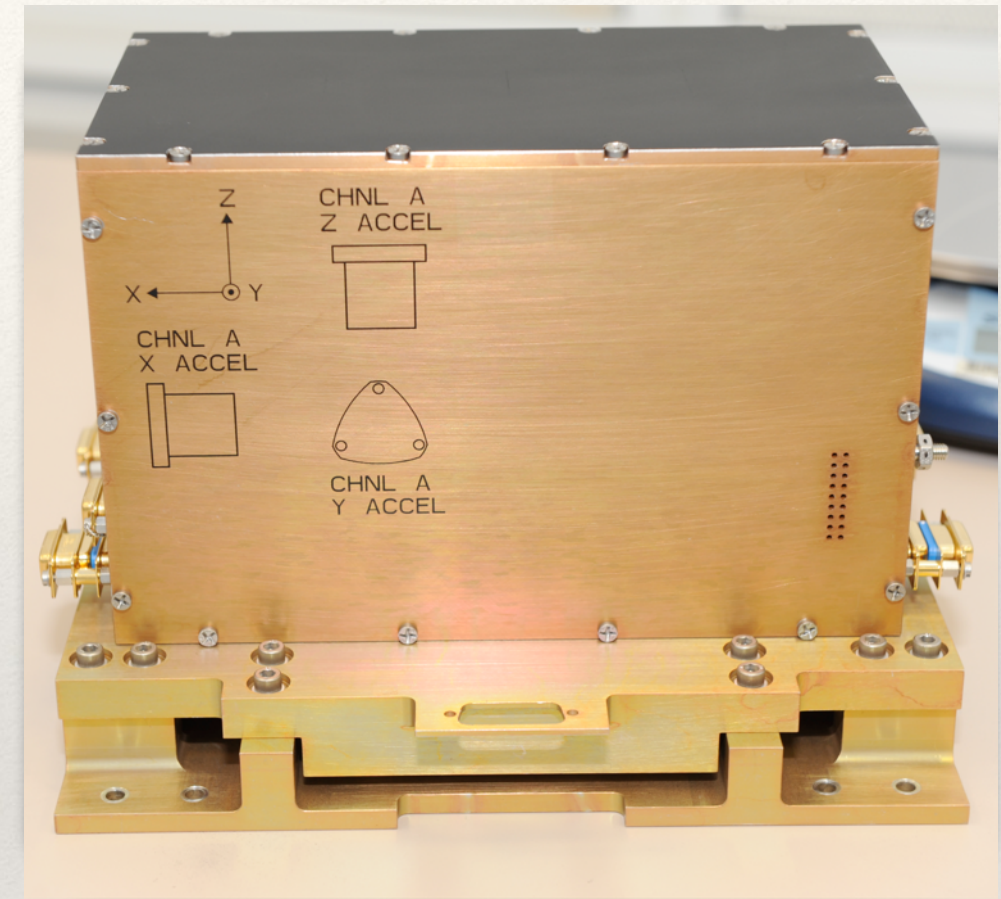
without a gyro, knowledge of (an “effective” rigid-body) inertia tensor is required



Acceleration Measurement System

Acceleration Measurement System (AMS),
manufactured by ZIN Technologies

- three orthogonal Honeywell QA3000 accelerometers
- 100 kHz analog-to-digital sampling
- dynamic range of greater than $\pm 25,000 \mu\text{g}$
- resolution of less than $1 \mu\text{g}$
- short-term (1σ) bias stability over a twelve hour period of better than $1 \mu\text{g}$
- effective bandwidth of 250 Hz
- 1 KHz (down-sampled) acceleration integrated (corrected and summed) to produce an incremental velocity-change output at 4 Hz
- low-pass bias estimation filter





Accelerometer Model

Modeled as a proof-mass connected to a rigid-body by tri-axial springs, device acceleration relative to a body-fixed origin is

$$\mathbf{a}_d \equiv -\frac{k_d}{m_p} \boldsymbol{\xi} = \underset{b \leftarrow i}{\mathcal{A}} \left(\dot{\mathbf{V}}_o - \mathbf{a}_{\text{grav}} \right) + \dot{\boldsymbol{\omega}}^\times \mathbf{r}_d + \boldsymbol{\omega}^\times \boldsymbol{\omega}^\times \mathbf{r}_d$$

Introducing the base-body's center-of mass (\mathbf{r}_c) yields a **truth model**

$$\mathbf{a}_d = \frac{\mathbf{f}_t}{m} + \dot{\boldsymbol{\omega}}^\times \underbrace{(\mathbf{r}_d - \mathbf{r}_c)}_{\mathbf{r}_{cd}} + \boldsymbol{\omega}^\times \boldsymbol{\omega}^\times (\mathbf{r}_d - \mathbf{r}_c) - \underbrace{(2 \cdot \boldsymbol{\omega}^\times \dot{\mathbf{r}}_c + \ddot{\mathbf{r}}_c)}_{\text{multi-body effects}}$$

where \mathbf{f}_t is the acceleration due to body-fixed thrusters.

Acceleration measurement model assumes n uni-axial measurements (along \mathbf{u}_n) corrupted by bias, noise and scale factor errors

$$\mathbf{a}_k = \begin{bmatrix} a_x \\ a_y \\ a_z \end{bmatrix}_{t_k} = \underbrace{(\mathcal{O}^\top \mathcal{O})^{-1} \mathcal{O}^\top}_{\text{pseudo-inverse of orthogonality matrix}} \left\{ \begin{bmatrix} (1 + \delta\kappa_1) \hat{\mathbf{u}}_1^\top \\ (1 + \delta\kappa_2) \hat{\mathbf{u}}_2^\top \\ \vdots \\ (1 + \delta\kappa_n) \hat{\mathbf{u}}_n^\top \end{bmatrix} \mathbf{a}_d + \begin{bmatrix} b_1 \\ b_2 \\ \vdots \\ b_n \end{bmatrix} + \begin{bmatrix} \eta_1 \\ \eta_2 \\ \vdots \\ \eta_n \end{bmatrix} \right\}$$



Velocity Estimation

“Effective” integration of the measurement yields

$$\int_{t_1}^{t_2} \mathcal{A}_{i \leftarrow b} \mathbf{a}_k d\tau = \int_{t_1}^{t_2} \mathcal{A}_{i \leftarrow b} \frac{\mathbf{f}_t}{m} d\tau + \int_{t_1}^{t_2} \mathcal{A}_{i \leftarrow b} (\dot{\boldsymbol{\omega}}^\times \mathbf{r}_{cd} + \boldsymbol{\omega}^\times \boldsymbol{\omega}^\times \mathbf{r}_{cd}) d\tau - \int_{t_1}^{t_2} \mathcal{A}_{i \leftarrow b} (2 \cdot \boldsymbol{\omega}^\times \dot{\mathbf{r}}_c + \ddot{\mathbf{r}}_c) d\tau + \int_{t_1}^{t_2} \mathcal{A}_{i \leftarrow b} \mathbf{b} d\tau + \int_{t_1}^{t_2} \mathcal{A}_{i \leftarrow b} \boldsymbol{\eta} d\tau$$

Recognizing that the integrated thrust is the true quantity of interest (i.e. the velocity change of the spacecraft’s center-of-mass), the expression may be rearranged as

$$\underbrace{\Delta \mathbf{v}_c(t_1, t_2)}_{\text{truth states}} = \underbrace{\int_{t_1}^{t_2} \mathcal{A}_{i \leftarrow b} \mathbf{a}_k d\tau}_{\text{measurement}} + \underbrace{\left\{ \mathcal{A}_{i \leftarrow b} \boldsymbol{\omega}^\times \mathbf{r}_{cd} - \mathcal{A}_{i \leftarrow b} \dot{\mathbf{r}}_c \right\}}_{\text{centripetal}}^{t_2} - \underbrace{\int_{t_1}^{t_2} \mathcal{A}_{i \leftarrow b} \mathbf{b} d\tau}_{\text{bias}} - \underbrace{\int_{t_1}^{t_2} \mathcal{A}_{i \leftarrow b} \boldsymbol{\eta} d\tau}_{\text{noise}}$$

The first term on the left-hand side is provided directly from the AMS. The remaining terms must be either corrected by an estimated compensation, or tolerated in the performance.



AMS Measurement Corrections

Discrete approximation to measurement integral with sculling correction for frame rotation

$$\int_{t_1}^{t_2} \mathcal{A}_{i \leftarrow b}(\tau) \mathbf{a}_k d\tau \approx \sum_{i=250}^{250} \sum_{k=1}^{250} \mathcal{A}_{250 \leftarrow k}(\hat{\boldsymbol{\omega}}, k) \cdot \mathbf{a}_k \cdot (t_k - t_{k-1})$$

$$\mathcal{A}_{250 \leftarrow k}(\hat{\mathbf{e}}, \Phi_k) = \mathbb{I} - \sin \Phi_k \hat{\mathbf{e}}^\times + (1 - \cos \Phi_k) \hat{\mathbf{e}}^\times \hat{\mathbf{e}}^\times$$

$$\Phi_k = \|\hat{\boldsymbol{\omega}}\| \cdot \Delta t_k = \|\hat{\boldsymbol{\omega}}\| \cdot \frac{250 - k}{1000}$$

two-hundred fifty (1 Khz) acceleration samples produce a single 4 Hz velocity-increment in the frame of the final (250th) sample



Centripetal Compensation

Estimating the kinetic effect of having the accelerometers offset from the effective spin-center

$$E \left[\left\{ \underset{i \leftarrow b}{\mathcal{A}} [\boldsymbol{\omega}]^{\times} \mathbf{r}_{cd} \right\}_{t_1}^{t_2} \right] = \underset{i \leftarrow b_2}{\hat{\mathcal{A}}} [\hat{\boldsymbol{\omega}}(t_2)]^{\times} \hat{\mathbf{r}}_{cd}(t_2) - \underset{i \leftarrow b_1}{\hat{\mathcal{A}}} [\hat{\boldsymbol{\omega}}(t_1)]^{\times} \hat{\mathbf{r}}_{cd}(t_1)$$

Could be an exact correction, over an arbitrarily long time interval, but requires:

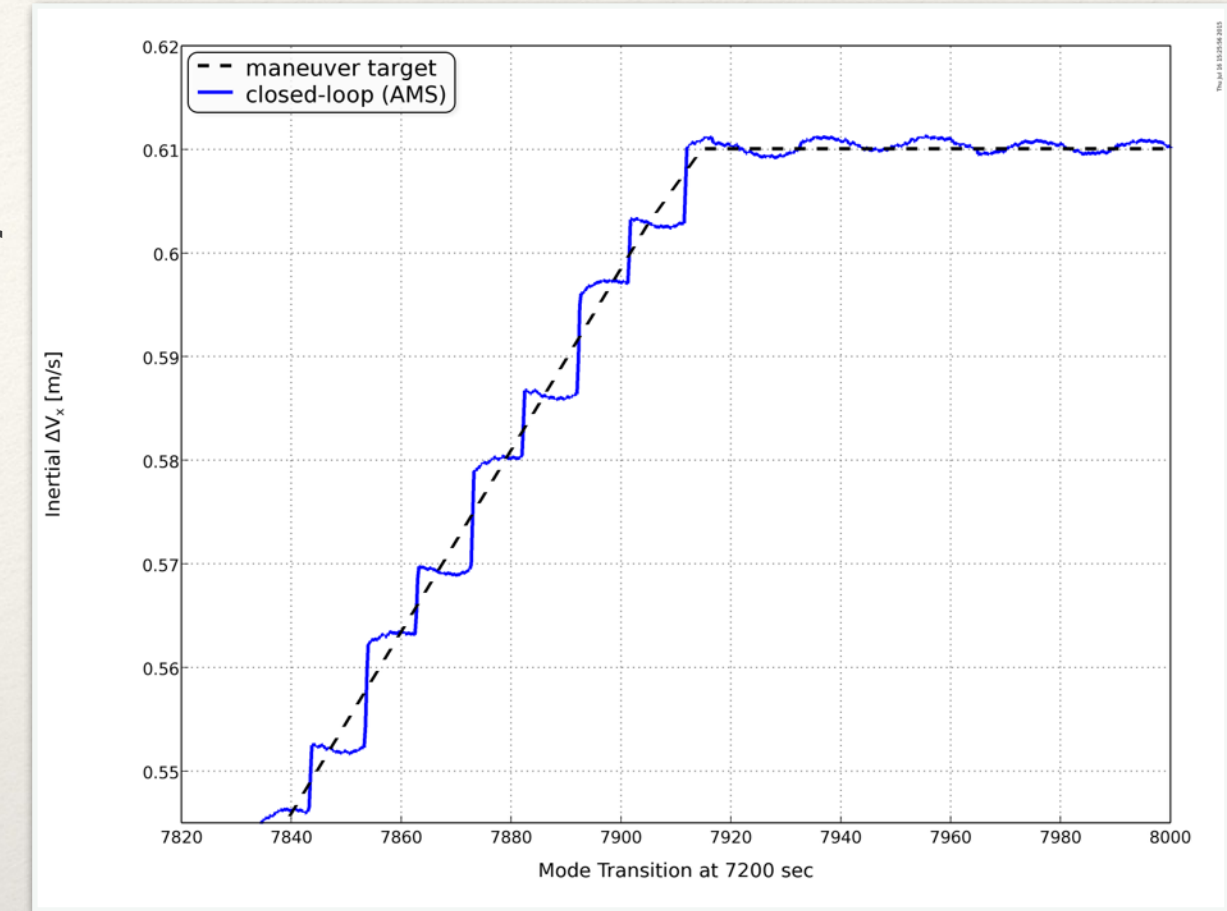
- good rate estimates (despite a rigid-body approximation)
- good knowledge of the spacecraft's center-of-mass (CM)
- sensor-head offsets are handled properly
- multi-body and structural (flex) dynamics (e.g. CM motion) integrates to zero over a sufficiently long duration since it is non-propulsive
- other error sources are small (e.g. non-linearity, scale factor, etc.) or well managed (e.g. thermal)



Velocity Controller

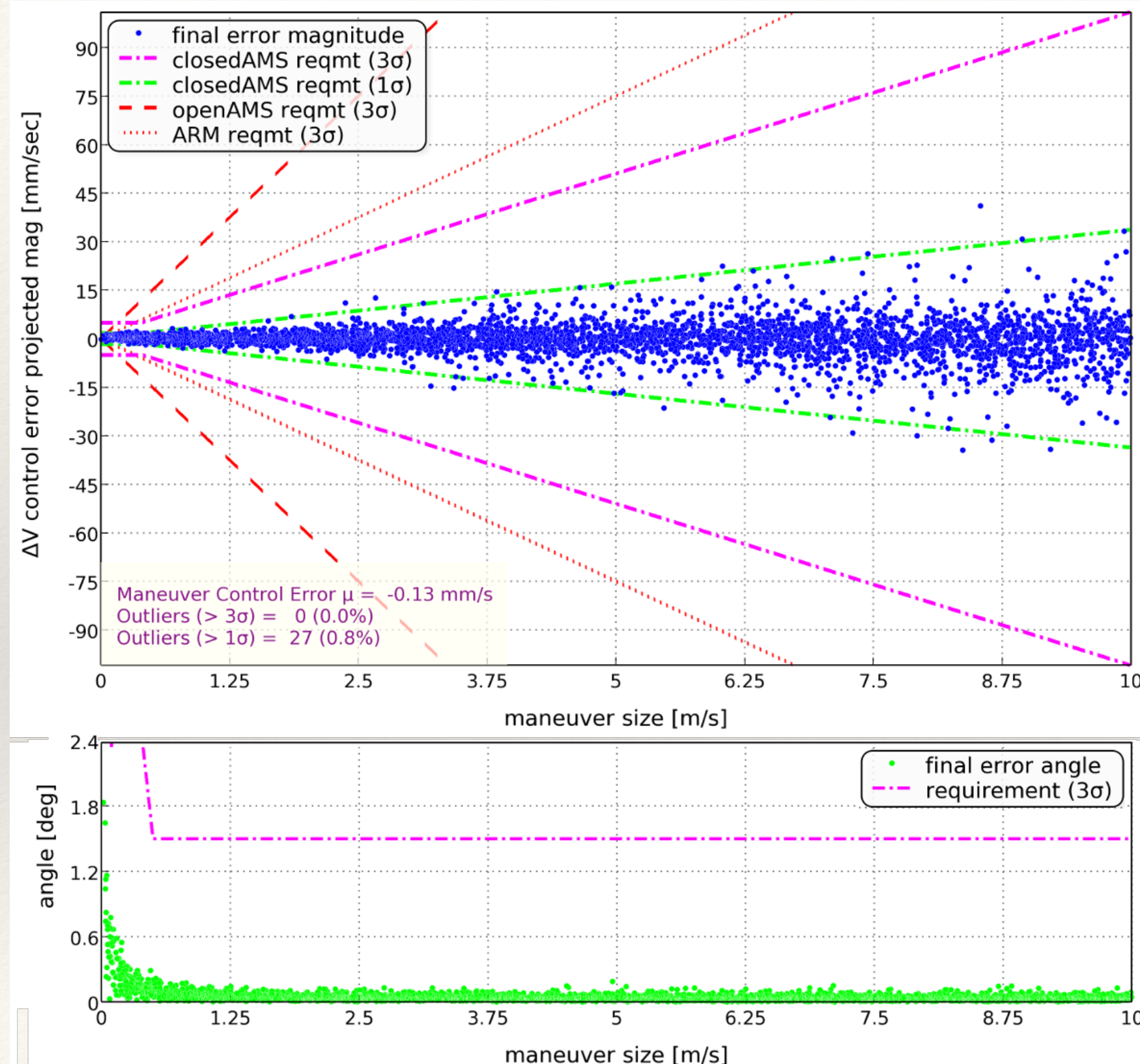
Classic tracker design

- time-varying inertial target table uploaded prior to each maneuver
- incremental-velocity feedback from AMS is accumulated in inertial space by the ACS
- Δv error is projected onto the axial and radial thrusters
- axial thrust can be continuous
- radial thrust must be pulsed to correspond with the two banks of thrusters spinning into inertial alignment (an iterative solver is employed to achieve precise pulse-centering)
- momentum control is interleaved to maintain pointing-direction, spin-rate, and minimal nutation
- wire-boom excitation is typically less than 2° out-of-plane and 4° in-plane





System Robustness

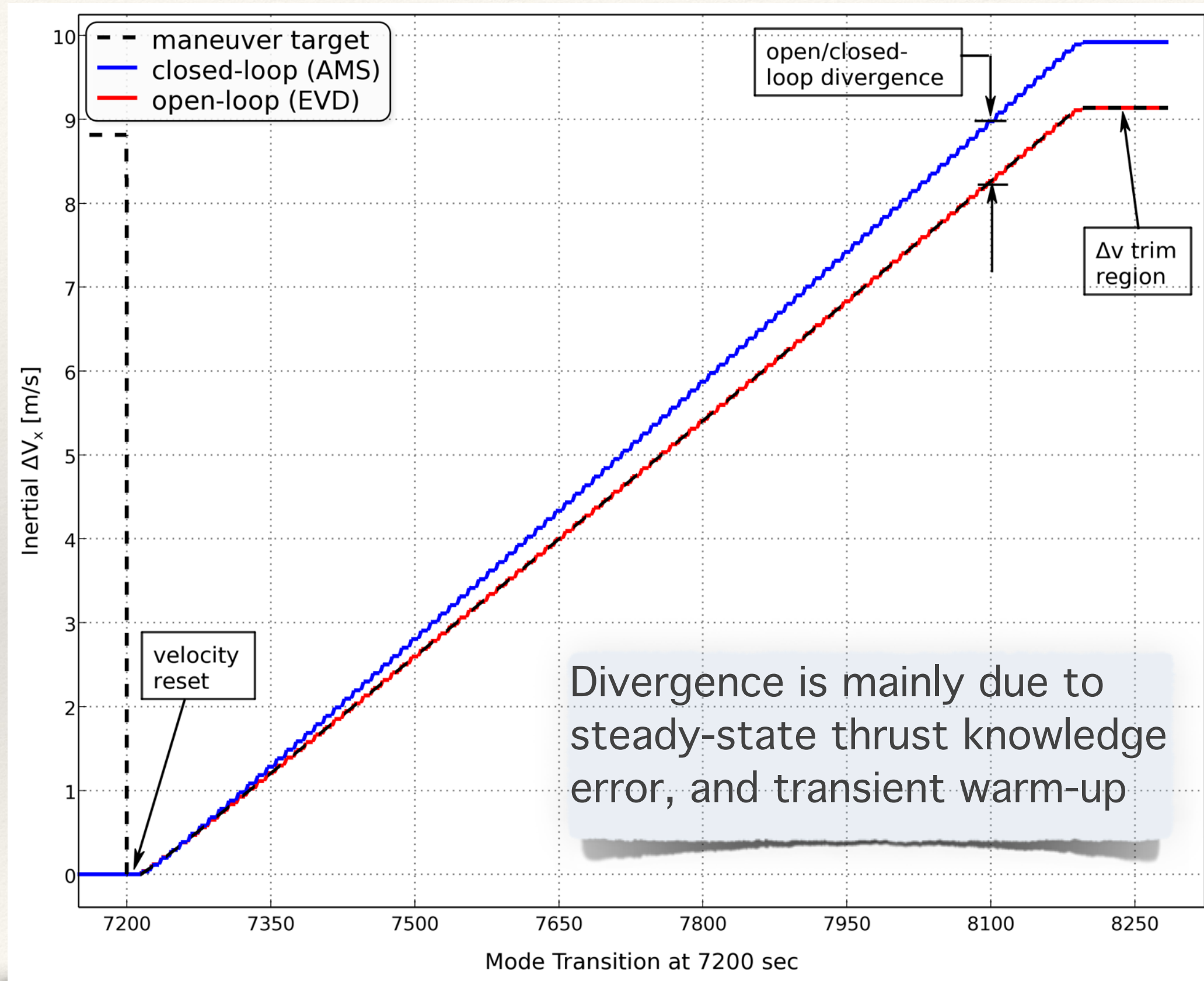


Verified system performance using Monte Carlo methods with a high-fidelity non-linear time-domain simulation.

A 99% confidence (1% consumer risk) requires zero failures to meet performance requirement in 3410 samples.



Open-Loop Flight Performance





Closed-Loop Flight Performance

Verified change in semi-major axis (SMA) using GPS- Enhanced Onboard Navigation System (GEONS) which is producing 5-meters (3σ) accuracy.

Maneuver (DOY)	Obs ID	Final Target Magnitude mm/s	GEONS Solution Semi-major Axis Δ -error	Final Servo-Error		AMS Bias Estimate (μ g)		
				mm/s	% target	X	Y	Z
GS-095 (166,167)	1	118.6	-1.14%	1.5	1.25%	114.7	78.9	49.6
	2	18.3	-0.57%	1.0	5.73%	94.3	93.9	47.3
	3	46.9	-0.73%	1.1	2.27%	75.2	92.5	140.1
	4	77.0	0.55%	1.1	1.44%	108.3	96.1	125.1
FI-116 (188)	1	0	—	—	—	115.3	77.4	49.7
	2	4077.5	-0.79%	1.0	0.03%	95.0	94.0	47.5
	3	9175.6	-0.26%	0.2	0.00%	76.9	94.3	140.9
	4	4452.1	-0.26%	1.2	0.03%	107.2	93.9	125.4
FI-119 (190)	1	0	—	—	—	—	—	—
	2	3511.6	-0.61%	0.8	0.02%	93.7	94.0	47.6
	3	4149.7	-0.18%	1.3	0.03%	76.9	94.7	140.8
	4	6068.7	-0.27%	1.3	0.02%	106.9	95.5	125.3